Colloid Cysts of the Third Ventricle: Correlation of MR and CT Findings with Histology and Chemical Analysis

Philippe P. Maeder[1]
Stig L. Holtås[1]
L. Nihal Basibüyük[1]
Leif G. Salford[2]
U. A. Staffan Tapper[3]
Arne Brun[4]

Eight patients with colloid cysts of the third ventricle were examined with CT and MR. In six, surgical resection was performed and the material was subjected to histologic evaluation; the concentrations of trace elements were determined by particle-induced X-ray emission. Stereotaxic aspiration was performed in two. The investigation showed that colloid cysts are often iso- or hypodense relative to brain on CT (5/8), but sometimes have a center of increased density. Increased density did not correlate with increased concentration of calcium or other metals but did correlate with high cholesterol content. Colloid cysts appear more heterogeneous on MR (6/8) than on CT (3/8), despite a homogeneous appearance at histology. High signal on short TR/TE sequences is correlated with a high cholesterol content. A marked shortening of the T2 relaxation time is often noticed in the central part of the cyst. Analysis of trace elements showed that this phenomenon is not related to the presence of metals with paramagnetic effects.

Our analysis of the contents of colloid cysts does not support the theory that differing metallic concentrations are responsible for differences in MR signal intensity or CT density. We did find that increased CT density and high MR signal correlated with high cholesterol content.

***AJNR* 11:575–581, May/June 1990; *AJR* 155: July 1990**

Colloid cysts of the third ventricle, which represent the best known form of neuroepithelial cyst, are rare tumors (0.25–0.5% of all intracranial tumors [1, 2]). The origin of this benign pathologic structure has been controversial, but since the work of Shuangshoti et al. (1965–1966) [3, 4], the most widely accepted theory suggests an origin in the primitive neuroepithelium of the tela choroidea. Neuroepithelial cysts are also found in the lateral ventricles; this has been documented in many cases at autopsy [3], but the cysts have been visualized rarely on CT and MR [5].

It can be assumed that the very strategic position of a colloid cyst in the anterior part of the third ventricle, allowing it to obstruct one or both foramina of Monro, thus creating acute hydrocephalus, probably accounts for the more common recognition of cysts in this location and descriptions in the clinical and radiologic literature. Before CT, ventriculography and encephalography could establish the correct diagnosis, but did not provide any information about the content of the cysts. With the introduction of CT, the interest of radiologists was aroused by the very polymorphous appearance of these lesions, which were reported as hypo- [6], iso- [7], or, more commonly, very hyperdense relative to brain parenchyma [8–10]. The explanation for the increased density has only rarely been found to be hemorrhage [11] or gross calcification [7]. Therefore, several hypotheses have been proposed concerning the content of iron or other radiodense ions in the secretion products of the cyst [9, 12]. Reports on the contrast enhancement of these lesions, particularly in the periphery or capsule, have been contradictory.

The signal pattern of colloid cysts on MR has also been described as heterogeneous [13–15]. A few cases have been reported, showing different components in

Received June 22, 1989; revision requested August 3, 1989; revision received November 1, 1989; accepted November 16, 1989.

This work was supported by grants from the Swedish Medical Research Council (B89-39X-08164-03A) and the Crafoord Foundation, Lund.

[1] Department of Diagnostic Radiology, University Hospital, S-221 85 Lund, Sweden. Address reprint requests to S. Holtås.

[2] Department of Neurosurgery, University Hospital, S-221 85 Lund, Sweden.

[3] Department of Nuclear Physics, Lund Institute of Science and Technology, Lund, Sweden.

[4] Department of Pathology, University Hospital, S-221 85, Lund, Sweden.

0195-6108/90/1103-0575

the so-called colloid matrix of the cyst [14, 15]; it has been suggested that the unusual signal pattern is caused by the inclusion of paramagnetic material [16]. The aim of our study was to analyze the complex appearance of colloid cysts on MR and CT and to try to find an anatomic or chemical explanation for their peculiar and variable appearances.

Materials and Methods

Eight patients (seven men and one woman 30–74 years old) with colloid cysts of the third ventricle were studied from 1986 to 1988 with CT and MR. Histologic proof of the diagnosis was available in six patients. In two patients surgical and stereotaxic biopsy did not provide enough material for complete histologic analysis.

All patients underwent pre- and postcontrast CT examinations with a Toshiba TCT 80-B scanner. A bolus injection of 100 ml of iohexol was used for enhancement. Routinely, 10-mm-thick axial slices were obtained except in the posterior fossa, where 5-mm-thick slices were used. In some patients 5-mm-thick slices were also used in the region of the colloid cyst; in the three patients who underwent stereotaxic procedures, 2-mm-thick slices were obtained as well. In one case, 2-mm-thick coronal slices were obtained.

After separating homogeneous from nonhomogeneous cysts, the density of the different components of the content of the cyst was compared with that of brain parenchyma (thalamus) and classified on an arbitrary five-point scale: −2 = much lower density than brain parenchyma, −1 = lower density, 0 = isodense, +1 = higher density, and +2 = much higher density. The size and shape were determined, as well as contrast enhancement of the content or capsule of the cysts.

All MR examinations were performed on a 0.3-T Fonar β-3000M unit. Imaging was performed with a multislice technique using spin-echo (SE) sequences. A 256 × 256 matrix was used with a pixel size of 0.91–1.18 mm. The slice thickness varied between 4.5 and 7 mm. All patients had one short TR/TE and one long TR/TE sequence in the coronal and sagittal planes. Some patients were examined in the axial projection as well. The following parameters were used: for short TR/TE sequences, 600/30/2 (TR/TE/excitations) or 400/16/3; for long TR/TE sequences, 2000/85/1, 2000/60/1, or dual echo 1500/30–85/1.

We performed separate analyses of short and long TR/TE images; as for the CT analysis, we separated the cysts into homogeneous and nonhomogeneous groups and compared the intensity of the different components of the cysts with that of brain parenchyma (thalamus) according to the same arbitrary five-point scale.

Surgical extirpation was performed in six cases and stereotaxic biopsy in three (both procedures were performed in one patient). Pathologic examination was performed in six cases (H and E–stained 5-μm-thick sections). Special staining for iron (Gomori's method) was done in five cases; these studies were reviewed with special attention to cholesterol and calcium deposits. Cholesterol crystals have a typical appearance at histologic examination. The amount of cholesterol in the colloid stroma was estimated in each case by the number of typical spindle-shaped clefts. (The clefts are created when the cholesterol is dissolved by alcohol during the preparation.)

The content of six cysts was analyzed with quantitative measurements of trace elements with the particle-induced X-ray emission (PIXE) method [17]. By using this method, the concentrations of all elements with an atomic weight higher than sodium were measured, including metals with possible influence on MR images and CT scans, such as gadolinium, chromium, manganese, nickel, copper, iron, and calcium. The PIXE method has several advantages over the conventional atomic absorption method. It is multielemental and sensitive in small tissue samples with detection limits down to parts-per-million dry weight. The method was previously applied in a study of elemental differences between brain tumors and surrounding normal tissue [18]. The values for normal brain tissue from the previous study were used for comparison in the present study.

Results

CT

The results of the CT examinations are given in Table 1. The peripheral components of the content of the cysts could be divided into two groups: (1) those isodense or slightly hypodense relative to brain parenchyma (cases 1–5) (Figs. 1A and 2A) and (2) those hyperdense relative to brain parenchyma (cases 6–8) (Figs. 3A and 4A). In the first group, three

TABLE 1: MR Signal Intensity and CT Density of Colloid Cysts Relative to Brain Parenchyma

Case No.	Signal Intensity				CT Density		Cholesterol
	Short TR/TE		Long TR/TE				
1[a]	Periphery	0, −1	Periphery	+1, +2	Periphery	−1	Negative
	Center	+1	Center	−1	Center	+1	
2	Periphery	+1	Periphery	+2	Periphery	0	Negative
	Two dots	−1	Two dots	−2	Two dots	+1	
3	Periphery	0	Periphery	+2	Periphery	0	Negative
	Center	−1	Center	−2	Center	+1	
4	Homogeneous	0	Homogeneous	+2	Homogeneous	0	Not examined
5	Homogeneous	0	Periphery	+2	Homogeneous	0	? Positive
			Center	−1			
6	Periphery	+1	Periphery	0	Homogeneous	+2	Positive
	Center	0	Center	−2			
7	Periphery	+1	Periphery	0	Homogeneous	+2	Not examined
	Two dots	−1	Two dots	−1			
8	Homogeneous	+2	Homogeneous	−2	Homogeneous	+2	Positive

Note.—MR signal intensity and CT density were assessed relative to brain parenchyma (thalamus) on a scale of −2 to +2: −2 = much lower than brain; −1 = lower than brain; 0 = equal to brain; +1 = higher than brain; +2 = much higher than brain. Cholesterol content was examined by the histologic method.

[a] Fluid/fluid level in periphery.

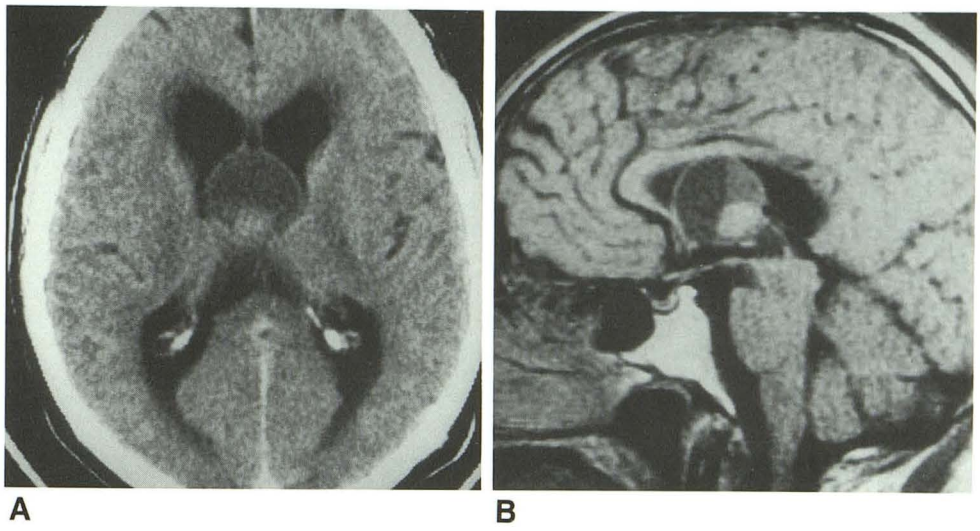

Fig. 1.—Case 1.
A, Unenhanced CT scan shows hypodense thin-walled cyst in anterosuperior part of third ventricle containing isodense posterior nodule.
B, Midline sagittal spin-echo MR image (600/30) shows fluid level in hypointense peripheral part of cyst. Posterior nodule is slightly hyperintense relative to brain parenchyma.
C, Coronal spin-echo (proton-density) MR image (1500/30) through posterior part of cyst shows slightly hyperintense signal from posterior fluid part of cyst. Nodule is isointense relative to brain parenchyma.
D, Coronal spin-echo MR image (1500/85) through posterior part of cyst shows very intense signal from peripheral part and low signal of nodule.

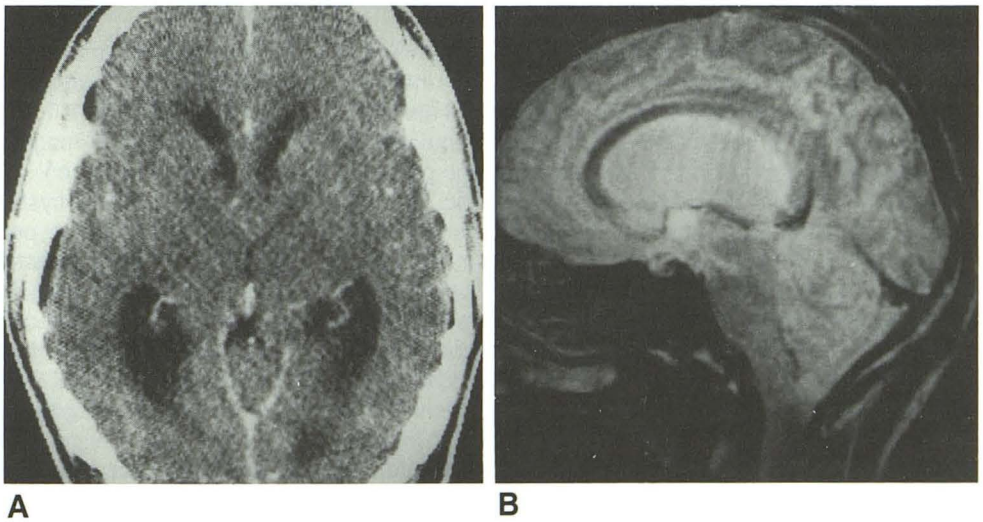

Fig. 2.—Case 5.
A, Contrast-enhanced CT scan shows very thin third ventricle and dilatation of lateral ventricles. No mass can be delineated in vicinity of foramen of Monro.
B, Midline sagittal spin-echo MR image (2000/85) shows hyperintense cyst in anterosuperior part of third ventricle.

cysts (cases 1–3) were heterogeneous (Fig. 1A), showing a second, more dense component usually located centrally or in the lower part in the direction of gravity.

The size of the cysts ranged from 5 to 30 mm in diameter; their shape had a tendency to become oval or less rounded as they became bigger. One cyst could not be measured because it was isodense relative to brain tissue and did not enhance.

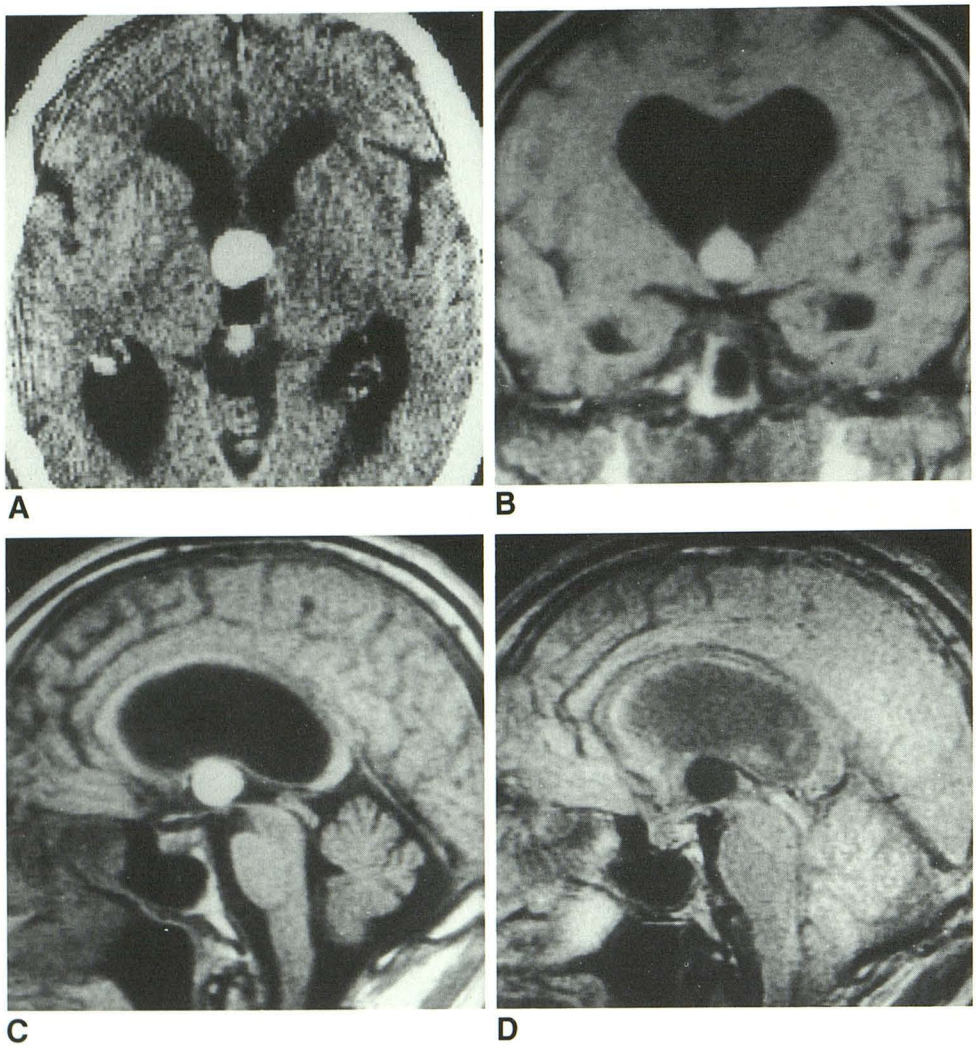

Fig. 3.—Case 8.
***A*, Unenhanced CT scan shows very hyperdense mass in anterosuperior third ventricle.**
***B* and *C*, Coronal (*B*) and midline sagittal (*C*) spin-echo MR images (400/16) show homogeneous intense mass in anterosuperior third ventricle.**
***D*, Midline sagittal spin-echo MR image (2000/60) shows homogeneous very low signal from mass in anterosuperior third ventricle.**

A very thin rim of contrast enhancement was observed in one case, probably representing the capsule of the cyst. Otherwise, no enhancement could be seen in any of the cysts. In the two cases of isodense cysts, the third ventricle was very thin, which is a secondary sign indicating the presence of the cyst (Fig. 2). All patients were hydrocephalic.

MR Imaging

The results of the MR examination are given in Table 1. The short TR/TE images showed less homogeneity in the content of the cysts than CT scans did (five cysts being heterogeneous), but the appearance in the peripheral part of the cyst was very similar to the CT findings in all but one case. The peripheral components could be divided into two equal groups of four iso- or slightly hypointense cysts (cases 1 and 3–5) (Figs. 1B and 1C) and four hyperintense cysts (cases 2 and 6–8) (Figs. 3B, 3C, 4B, and 4C).

The largest of the cysts (case 1) showed a fluid/fluid level in its main part (Fig. 1). All central dense parts found on CT could be seen on MR as appearing iso- or hypointense relative to brain parenchyma; similar structures could be seen in two other hyperintense cysts that could not be seen on CT (Figs. 4B and 4C).

The long TR/TE images showed an almost exact reversal of the pattern seen on short TR/TE images, at least in the peripheral part of the cysts. All the iso- or slightly hypointense cysts turned brightly hyperintense (Figs. 1D and 2B), and all except one of the hyperintense cysts turned iso- or hypointense (Figs. 3D and 4D).

The behavior of the central parts was the most striking; they all became more hypointense on long TR/TE images than on short TR/TE images, some of them even in an extreme way, raising the suspicion of a paramagnetic effect (Fig. 4D).

One cyst, the only one to appear homogeneous on all imaging studies (case 8, Fig. 3), demonstrated a remarkable reduction in the signal intensity of its entire content on long TR/TE images, as if the substance responsible for the effect was spread diffusely in the colloid matrix, contrary to the pattern in all the other cysts.

The size and shape of the cysts were measured more easily

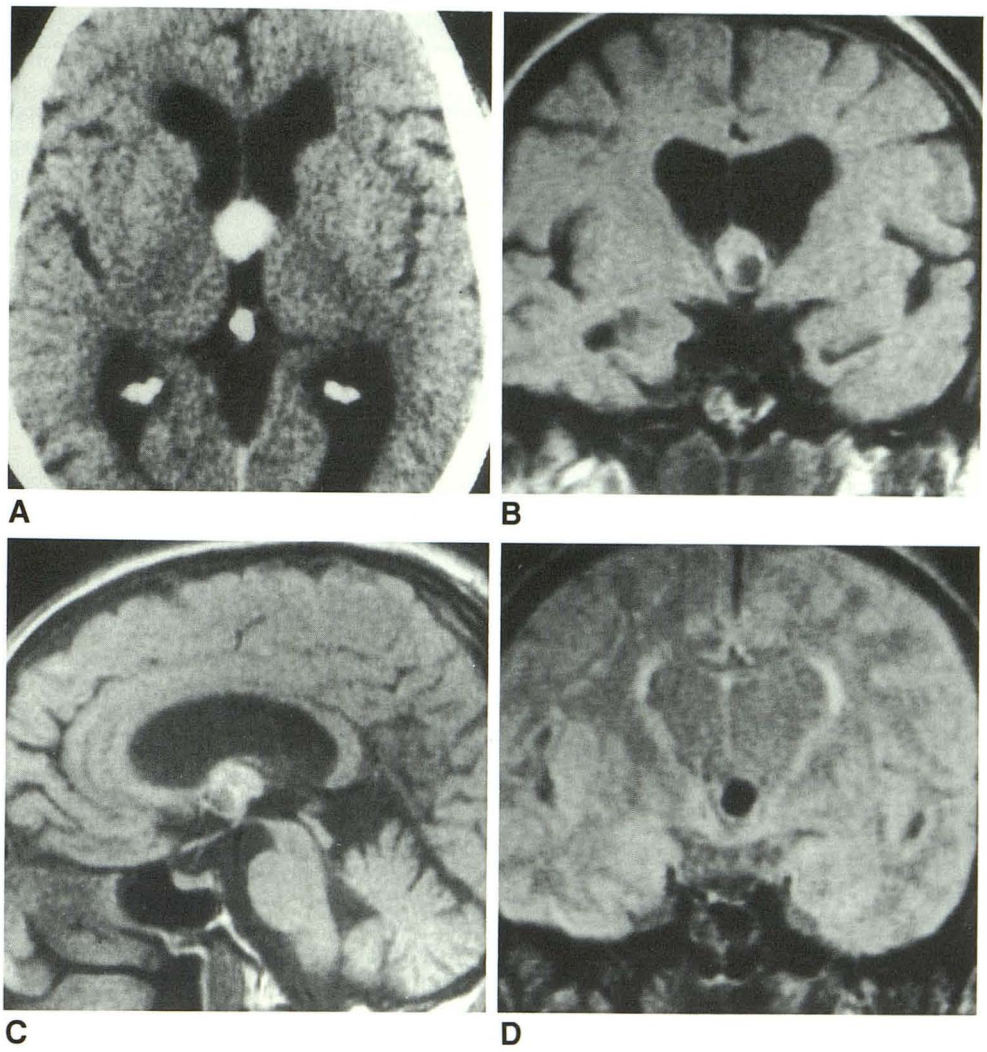

Fig. 4.—Case 6.
***A*, Unenhanced CT scan shows homogeneous hyperintense mass in anterosuperior third ventricle.**
***B* and *C*, Coronal (*B*) and midline sagittal (*C*) spin-echo MR images (600/30) show intense signal from peripheral and superior part of cyst. Smaller centrally and caudally located part has lower signal than brain parenchyma.**
***D*, Coronal spin-echo MR image (2000/60). Signal in peripheral and superior part of cyst is isointense relative to brain parenchyma. Central part is very hypointense.**

and accurately on MR than on CT. In two cases of isodense cysts on CT, the lesions were seen clearly only on MR (cases 4 and 5). In one case the peripheral part was seen only on MR (case 3).

Histopathology

The cysts removed in toto always had a thin wall consisting of an inner layer of cuboidal or cylindrical cells and an outer layer of connective tissue including vessels. The inner content of the cysts was a homogeneous, amorphous eosinophilic substance with a few cells mostly of the macrophage type. No anatomic structure corresponding to the inner and outer parts seen on MR and CT could be identified.

In three cases, no cholesterol crystals were found. Two cases were clearly positive; in a third case the amount of stereotaxically removed material was very small and of bad quality, which impaired the estimation of cholesterol content (Table 1).

Iron staining did not show iron in the colloid, but small quantities were found in macrophages in the cyst walls and around vessels in cases 1, 3, 6, and 8. There were no signs of recent or old hemorrhage. No calcification was observed in the colloid stroma or cyst wall.

Elemental Analysis

There were wide variations in the concentrations of different trace elements in the colloid of the cysts. The concentrations of the elements most interesting in MR and CT are given in Table 2. Calcium was significantly increased (two to eight times) in the tissue samples compared with the concentration in normal brain ($p < .01$, Wilcoxon Rank Sum Test). However, the increased calcium concentration did not correlate with increased density on CT, since the highest value was found in an isodense cyst (case 5) and the lowest in a strongly hyperdense cyst (case 6).

When evaluating the other elements of interest as a group, there were no significant differences from normal brain tissue. When looking at individual values of the paramagnetic elements, no pattern could be found supporting the theory that a paramagnetic effect of the metals was the cause of the

TABLE 2: Concentration of Trace Elements in Tissue Samples of Colloid Cysts

Case No.	Element (μg/g dry material)						
	Calcium	Chromium	Manganese	Iron	Nickel	Copper	Gadolinium
1	1540	–	24.1	18	4.3	9.7	–
2	990	–	–	54	0.9	60.6	–
3	1200	–	2.0	351	–	5.9	–
5	2920	–	–	225	43.6	23	–
6	640	–	–	37	–	13.6	–
7	1120	–	2.8	45	–	9.5	–
Normal brain	350	–	1.7	260	–	19	–

Note.—Only elements of interest in MR and CT imaging are recorded. Dash (–) denotes below detection level (ppm). Normal values are given for comparison [18]. Concentration of calcium is significantly higher in tissue samples than in normal brain ($p < .01$); otherwise, no significant differences were found.

signal pattern on MR. The concentration of iron was lower in all colloid samples than in normal brain, except in case 3, where it was somewhat elevated. Thus, the low signal (T2-shortening) in the central part of the cyst seen in cases 2, 3, 6, and 8 (Table 1) could not be explained by the presence of iron.

Discussion

Several reports describe the appearance of colloid cysts of the third ventricle on CT [2, 5–11]. Most reports of MR studies describe single or a few cases [5, 14–16, 19] and do not include analysis of the content of the cysts. Moreover, there is some controversy about the density, contrast enhancement, signal pattern on MR, and homogeneity of the cysts. In our study, the majority of cysts (5/8) were of low density on CT, although some of them had components in the central part of increased density. Only three of eight were homogeneously hyperdense. Two of these, which were evaluated histologically, showed a high cholesterol content. Cysts of low density in their peripheral part had a low cholesterol content at analysis. The high density could not be explained by high calcium content or high concentrations of other metals, as shown by the different analyses performed (Tables 1 and 2). Thus, the high density must be explained by other factors; that is, increased electron density in the cyst material, as suggested by Isherwood et al. [20]. It was possible to evaluate the isodense parts of the cysts only after their presence became known as a result of the MR examination. Unlike other authors [7, 9], we did not find any case exhibiting contrast enhancement of the cyst material. However, in one patient, enhancement of the thin capsule was observed (case 4). In cases of isodense cysts there might be diagnostic difficulties. However, dilatation of the lateral ventricles in combination with a small third ventricle should lead to the correct diagnosis, as occurred in two of our cases (Fig. 2).

The heterogeneous appearance of the colloid cysts was more apparent on MR than on CT. Only two cysts in our material were homogeneous on all sequences. The heterogeneous appearance is not caused by any anatomic structures since all cysts showed a uniform amorphous matrix surrounded by a thin capsule at histologic examination. The capsule is much too thin to represent the outer rim seen on MR, which has signal characteristics different from that of the center. The different signal patterns must then be explained by different chemical composition or a concentration gradient in the cyst. The high signal seen in the peripheral part on short TR/TE SE sequences in four cases might be explained by high cholesterol content, as has been described in craniopharyngiomas and Rathke cleft cysts [21, 22], since two of the three cases examined had high cholesterol at histologic examination. In two cases with low signal in the peripheral part that were examined histologically, no cholesterol was found. However, in the third case with moderately increased signal on short TR/TE images, no high cholesterol content was found, and the high signal is therefore difficult to explain. The signal from the peripheral part showed a reversed pattern on long TR/TE SE sequences in all cases except one in which a slightly increased signal on the short TR/TE sequence became more intense on the long TR/TE sequence. This was the same case (case 2) in which no cholesterol was found despite somewhat increased signal on short TR/TE images. The strong signal seen on long TR/TE SE sequences in cases of low signal on short TR/TE SE sequences in the peripheral part of the cyst could be explained by a protein-containing mucus in the cysts.

The signal from the central part of the heterogeneous cysts showed an unusual pattern and was actually the reason why this study was initiated. All patients had low signal from this part of the cyst on long TR/TE SE sequences. In some cases the signal reduction was marked (Fig. 4D). On short TR/TE SE sequences the signal intensity was always stronger. This pattern has been observed by other authors, and it has been suggested that it could be caused by paramagnetic effects from metallic content in the cyst [16]. Our analysis of the cyst material does not support this theory, since we found no increase in iron or other metals causing a shortening of the T2 relaxation time. Another possible explanation of this phenomenon might be the presence of chemical compounds with free radicals [23, 24]. This mechanism has been suggested as the explanation of the shortening of T1 and T2 relaxation caused by the melanin in melanotic melanoma [25].

In summary, colloid cysts are often iso- or hypodense relative to brain on CT but sometimes have a center of increased density. There is a correlation between CT density and cholesterol content. The increase in density on CT is not

caused by calcium or other metals. Colloid cysts most often appear heterogeneous on MR despite a homogeneous appearance at histology. This phenomenon is supposed to be caused by different chemical compositions or a concentration gradient in the cysts. High cholesterol content is associated with high signal on short TR/TE SE sequences. A marked shortening of the T2 relaxation is often noted in the center of the cyst. This phenomenon is not caused by the presence of metals with paramagnetic effects.

ACKNOWLEDGMENT

Ann-Christin Ekholm is acknowledged for her assistance during the PIXE analysis.

REFERENCES

1. Kazner E, Wende S, Grumme T, Lanksch W, Stochdorph O. *Computed tomography in intracranial tumors. Differential diagnosis and clinical aspects.* Heidelberg: Springer-Verlag, **1982**
2. Guner M, Shaw MDM, Turner JW, Steven JL. Computed tomography in the diagnosis of colloid cyst. *Surg Neurol* **1976**;6:345–348
3. Shuangshoti S, Netsky MG. Neuroepithelial (colloid) cysts of the nervous system. Further observations on pathogenesis, location, incidence, and histochemistry. *Neurology* **1966**;16:887–903
4. Shuangshoti S, Roberts MP, Netsky MB. Neuroepithelial (colloid) cysts. Pathogenesis and relation to choroid plexus and ependyma. *Arch Pathol Lab Med* **1965**;80:214–223
5. Czervionke LF, Daniels DL, Meyer GA, Pojunas KW, Williams AL, Haughton VM. Neuroepithelial cysts of the lateral ventricles: MR appearance. *AJNR* **1987**;8:609–613
6. Hine AL, Chui MS. Hypodense colloid cyst of the third ventricle. *J Can Assoc Radiol* **1987**;38:288–291
7. Michels LG, Rutz D. Colloid cysts of the third ventricle. A radiologic-pathologic correlation. *Arch Neurol* **1982**;39:640–643
8. Sackett JF, Messina AV, Petito CK. Computed tomography and magnification angiotomography in the diagnosis of colloid cysts of the third ventricle. *Radiology* **1975**;116:95–100
9. Ganti SR, Antunes JL, Louis KM, Hilal SK. Computed tomography in the diagnosis of colloid cysts of the third ventricle. *Radiology* **1981**;138:385–391
10. Rivas JJ, Lobato RD. CT-assisted stereotaxic aspiration of colloid cysts of the third ventricle. *J Neurosurg* **1985**;62:238–242
11. Malik GM, Horoupian DS, Boulos RS. Hemorrhagic (colloid) cyst of the third ventricle and episodic neurologic deficits. *Surg Neurol* **1980**;13:73–77
12. Donaldson JO, Simon RH. Radiodense ions within a third ventricular colloid cyst. *Arch Neurol* **1980**;37:246
13. Roosen N, Gahlen D, Stork W, et al. Magnetic resonance imaging of colloid cysts of the third ventricle. *Neuroradiology* **1987**;29:10–14
14. Gowin W, Mariss G. Erscheinungsbild einer Kolloidzyste im dritten Ventrikel im magnetischen Resonanztomogramm (MRT). *ROFO* **1986**;145:723–725
15. Waggenspack GA, Guinto FC Jr. MR and CT of masses of the anterosuperior third ventricle. *AJNR* **1989**;10:105–110
16. Scotti G, Scialfa G, Colombo N, Landoni L. MR in the diagnosis of colloid cysts of the third ventricle. *AJNR* **1987**;8:370–372
17. Johansson SAE, Campbell IL. *PIXE: a novel technique for elemental analysis.* New York: Wiley, **1988**
18. Tapper UAS, Malmqvist KG, Brun A, Salford LG. Elemental regional distribution in human brain tumours—PIXE analysis of biopsy and autopsy samples. *Nucl Instrum Methods Phys Res* **1987**;B22:176–178
19. Kjos BO, Brant-Zawadzki M, Kucharczyk W, Kelly WM, Norman D, Newton TH. Cystic intracranial lesions: magnetic resonance imaging. *Radiology* **1985**;155:363–369
20. Isherwood I, Pullan BR, Rutherford RA, Strang FA. Electron density and atomic number determination by computed tomography. Part I: Methods and limitations. Part II: A study of colloid cysts. *Br J Radiol* **1977**;50:613–619
21. Kucharczyk W, Peck WW, Kelly WM, Norman D, Newton TH. Rathke cleft cysts: CT, MR imaging, and pathologic features. *Radiology* **1987**;165:491–495
22. Pusey E, Kortman KE, Flannigan BD, Tsuruda J, Bradley WG. MR of craniopharyngiomas: tumor delineation and characterization. *AJNR* **1987**;8:439–444, *AJR* **1987**;149:383–388
23. Brasch RC, London DA, Wesby GE, et al. Work in progress. Nuclear magnetic resonance study of a paramagnetic nitroxide contrast agent for enhancement of renal structures in experimental animals. *Radiology* **1983**;147:773–779
24. Brasch RC, Nitecki DE, Brant-Zawadzki M, et al. Brain nuclear magnetic resonance imaging enhanced by a paramagnetic nitroxide contrast agent: preliminary report. *AJR* **1983**;141:1019–1023
25. Gomori JM, Grossman RI, Shields JA, Augsburger JJ, Joseph PM, DeSimeone D. Choroidal melanomas: correlation of NMR spectroscopy and MR imaging. *Radiology* **1986**;158:443–445